AIAA 81-4161

Measurement of Derivatives for an Oscillating Airfoil with Flap

Valter J.E. Stark*
Saab Scania AB, Linköping, Sweden

By measuring forces and moments for $Re = 0.43 \times 10^6$ in two-dimensional flow in a water tunnel, the nine derivatives associated with plunge, pitch, and flap rotation have been determined for a NACA 64_2A015 profile with 42% flap. The test and the evaluation are briefly described and the derivatives are compared to results from a computer program based on inviscid thick-wing theory. Significant deviations, which are thought to be due mainly to viscous effects, were found in particular for flap moment due to unit plunge, pitch, and flap rotation and for lift and pitching moment due to unit flap rotation.

Nomenclature

- b = semichord = reference length. All quantities for which the dimension is length are made dimensionless by dividing by b
- C = stiffness of flap attachment
- f = dimensionless distance from flap hinge to the center of mass of the flap
- g_i = dimensionless distance from the node $x = x_i$ of the ith pitch mode to the flap hinge ($i = 1, 2$)
- H = dimensionless height of the tunnel test section
- h = dimensionless deflection at 25% chord
- K_{in} = force reaction from balances attached at $x = x_i$ in the nth test
- k_i = lift derivative = the limit of lift due to plunge ($i = a$), pitch ($i = b$), or flap rotation ($i = c$) divided by Qh, $Q\theta$, or $Q\beta$, respectively, for vanishing h, θ, and β
- M_{in} = moment reaction from balances attached at $x = x_i$ in the nth test
- m = mass of model
- m_f = mass of flap
- m_i = moment derivative = the limit of moment about quarter chord due to plunge ($i = a$), pitch ($i = b$), or flap rotation ($i = c$) divided by Qbh, $Qb\theta$, or $Qb\beta$, respectively, for vanishing h, θ, and β
- N = moment reaction from balances attached to the flap in test 2
- n_i = flap moment derivative = the limit of moment on the flap about the flap hinge due to plunge ($i = a$), pitch ($i = b$), or flap rotation ($i = c$) divided by Qbh, $Qb\theta$, or $Qb\beta$, respectively, for vanishing h, θ, and β
- Q = πqS, reference force
- q = $\rho U^2/2$, freestream dynamic pressure
- Re = $2Ub/\nu$, Reynolds number
- r_i = dimensionless radius of gyration for the model with respect to the node $x = x_i$ ($i = 1, 2$)
- r_f = dimensionless radius of gyration for the flap with respect to the flap hinge
- S = area of the model normal projection = reference area
- s_i = dimensionless distance from the node $x = x_i$ to the center of mass of the model ($i = 1, 2$)
- T = force reaction from balances attached to the flap in test 2
- U = freestream speed
- x = dimensionless streamwise coordinate with origin at quarter chord
- x_i = value of x at the node of the mode that corresponds to balances attached at the ith point
- β = flap angle
- θ = pitch angle
- ω = $\omega' b/U$, reduced frequency
- ω' = circular frequency
- ρ = fluid density
- μ = $m/(\pi\rho bS/2)$, mass ratio

Received Oct. 30, 1980; revision received March 9, 1981.

*Research Scientist. Member AIAA.

Introduction

FLUTTER problems may often be solved rather accurately by using aerodynamic forces from inviscid (thin-wing) theory, but in certain cases such as that of a wing with an oscillating control surface the viscous effects may be important. As the knowledge of the effect of viscosity in the unsteady case is very limited, the results of an investigation aimed at determining such effects will be described.

The investigation was performed by using a small water tunnel and a model with a simple flap spanning the test section. The flow was accordingly two-dimensional. Forces and moments on the model were determined by measuring the suspension reactions by strain gauge balances and by subtracting calculated inertial forces and moments.

A water tunnel was chosen partly because such a tunnel was available. This was inexpensive to operate and provided a Reynolds number satisfactorily large for an exploratory investigation. Amounting to 0.43×10^6 (based on the chord), the Reynolds number for which the measurements were made lies in the range 10^5 to 1.5×10^6 which contains the ranges treated in earlier low-speed investigations.[1-9,12] Furthermore, the use of a water tunnel implies a high value for the ratio of the aerodynamic forces to the model inertia forces which is favorable for the measurement accuracy.

Bratt and Scruton[1] performed corresponding measurements in a low-speed wind tunnel more than 40 yr ago. These were followed by similar tests by Silverstein and Joyner,[2] Reid and Vincenti,[3] Reid,[4] Bratt and Wight,[5] and Halfman.[6] Measurements for a profile with control surface were conducted by Drescher,[7] van de Vooren,[8] and Bergh.[9] Drescher used a water tunnel and measured the unsteady pressure on the model surface. The results of the early investigations were compared to thin-wing theory[10,11] predictions, while Spurk,[12] who conducted measurements for five special wing sections, employed thick-wing theory solutions of Küssner[13] for comparison.

The present results have been compared to derivatives calculated by a computer program[14] based on the same approach as that of Giesing[15] and applicable to a profile with a simple flap. As the viscosity is not allowed for in the program (except through the Kutta condition), the comparison should disclose viscous effects.

Method of Measurement

As the intention was to use stiff and sensitive semiconductor strain gauge balances, it was expected that accurate measurements could be made for amplitudes small enough for nonlinear contributions to be negligible. Therefore, it was not planned to perform measurements for pure plunging oscillations (which appears difficult) but instead for two pitching oscillations about two different axes (plus flap oscillations), because, in the linear case, the derivatives for plunge are determined by those for the two pitch motions. Sufficient data for evaluation of the nine derivatives that correspond to plunge, pitch, and flap rotation were obtained from three different tests.

In test 1, the flap was rigidly attached to the forward part or the main section of the model by very stiff connections, and

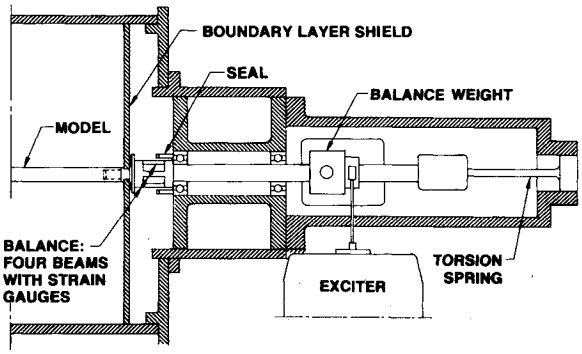

Fig. 1 Balance and excitation device.

Table 1 Values of certain constants

Quantity	Test 1 $i=1$	Test 1 $i=2$	Test 2 $i=1$	Test 3 $i=1$	Test 3 $i=2$
$C/(Qb)$	∞		0.	0.05025	
f	0.2740		0.2852	0.3006	
g_i	0.86	0.26	0.86	0.86	0.26
m_f/m	0.3247		0.3193	0.3132	
r_i^2	0.5367	0.2409	0.5343	0.5435	0.2464
r_f^2	0.1266		0.1319	0.1377	
s_i	0.5465	−0.0535	0.5493	0.5475	−0.0525
x_i	−0.2	0.4	−0.2	−0.2	0.4
x_H	0.66		0.66	0.66	
μ	0.8170		0.8129	0.8106	

the forward part was attached to two similar balances and excitation devices, one at each side of the tunnel. Similar measurements were made for the balances fastened to the model at two different locations, which yields oscillations about two different nodes $x=x_i, i=1, 2$.

In test 2, the flap was free from the forward part (no force or moment transmission) and instead connected to balances and excitation devices forming the flap hinge in this case. The forward part was attached (at $x=x_1$) to a second pair of balances rigidly fastened to the tunnel walls.

In test 3, the flap was attached to the forward part by cross springs (replacing the stiff connections in test 1), but otherwise test 3 was equal to test 1.

One of the excitation devices is shown in Fig. 1. It consists of a shaft that rests in special ball bearings and is connected to a torsion spring at one end. The balance at the other end was developed for the present purpose and contains semiconductor strain gauge elements. The problem of aligning the two devices was alleviated by attaching each balance to the model via a membrane.

The pitch angle in tests 1 and 3 and the flap angle in test 2 were measured by means of strain gauge elements on the torsion spring. This is possible since the shaft and the balances are stiff. Another method employing accelerometers in the model was also tried, but it was found less accurate, in particular for low frequencies.

The signals from the strain gauge elements were digitized by recording 24 values during each of two cycles of oscillation and by forming the arithmetic mean of corresponding values. Random errors were thereby neutralized to some extent. Coefficients in linear equations relating the force and moment signals to the desired quantities were determined by applying given static loads and moments. Checks through oscillations in still air and comparisons with calculated forces and moments were also made. A mirror and a laser beam were used for determining the coefficient in the linear relations for the flap and pitch angle. The recorded values were decomposed into Fourier components, but only the first-order component was used in the evaluation of the unsteady derivatives.

The model employed had a NACA 64_2A015 section with a trailing edge radius of 0.03 mm. The chord was 0.1 m, the flap chord 0.042 m, and the span 0.2 m. The slot separating the flap from the forward part was essentially bounded by coaxial cylindrical surfaces with radii differing by 0.3 mm. Boundary-layer shields were arranged at the model ends with slots between the model and the shields 0.3 mm wide. Other data and in particular those associated with the mass distribution are given in Table 1.

The tunnel employed, which is of the same design as one of the water tunnels described by Drescher,[16] has a test section height of 0.33 m. The tests were made at a freestream speed of 4 m/s and at a water temperature equal to the room temperature (about 23°C). The corresponding kinematic viscosity $\nu=0.0093$ g/cm·s/1 g/cm^3 $=0.0093$ cm^2/s and the Reynolds number $Re=2bU/\nu=0.43\times10^6$.

The transition point was fixed by means of steel balls 0.35 mm in diameter which were arranged along the 20% chord line on both sides of the airfoil. The spacing was 4 mm. Measurements for a boundary-layer trip containing a row of steel balls also along the 10% chord line on both sides were made as a check, but the changes in the results were small. The changes in the lift and moment due to pitch were not larger than 1%.

Data Reduction

Assuming small perturbations, we write the lift and moment increments that correspond to the deflection of the airfoil as linear combinations of h, θ, and β. The coefficients of these combinations may be called unsteady aerodynamic derivatives, for they are used and formed in a way similar to the derivatives employed in the fields of steady aerodynamics and stability of airplanes. It should be observed, however, that complex representation is required and that the unsteady derivatives are analytic functions of the complex reduced frequency $\eta+i\omega$; $\omega=\omega' b/U$. Only the harmonic case, $\eta=0$, is considered here.

The derivatives must be reduced to dimensionless counterparts for which the symbols k_a, k_b, k_c, m_a, m_b, m_c, n_a, n_b, and n_c may be used. These symbols, which were used by Küssner,[10] are so defined that the lift, the moment about 25% chord, and the flap moment about the hinge are given by $Q(k_a h+k_b\theta+k_c\beta)$, $Qb(m_a h+m_b\theta+m_c\beta)$, and $Qb(n_a h+n_b\theta+n_c\beta)$, respectively, where h is the dimensionless deflection at 25% chord and $Q=\pi qS$. The positive directions of the lift and moments are opposite to those of h, θ, and β, respectively, and h, θ, and β yield deflections in the same direction at the trailing edge.

The equations of motion of the model, which are required for evaluation of the unsteady derivatives, are most simply written in terms of derivatives referred to the node $x=x_i$ of the mode considered. These derivatives, which are denoted k_b^i, m_a^i, m_b^i, m_c^i, and n_b^i may be evaluated first. They can then be transformed into the Küssner derivatives by formulas given below.

The equations obtained by applying the two basic principles of dynamics to the model in test 1 may be reduced to

$$k_b^i=\mu\omega^2 s_i+K_{il}/(\theta Q) \tag{1}$$

and

$$m_b^i=\mu\omega^2 r_i^2+M_{il}/(\theta Qb) \tag{2}$$

where μ is the ratio of the model mass to the mass of a fluid cylinder with length and diameter equal to the model span and chord, respectively. The quantities K_{il} and M_{il} are the force and moment reactions from the balance pair in test 1. Their directions are shown in Fig. 2 ($n=1$).

In test 2, the forward part of the model is considered to be at rest because the balances are very stiff, the torsional stiffness being about 5000 Nm/rad. Separate applications of the basic principles of dynamics to the forward part and to the flap yield four equations from which the following formulas

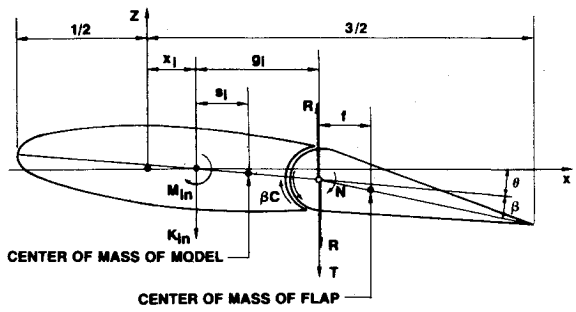

Fig. 2 Definition of symbols.

for derivatives k_c, m_c^l, and n_c may be derived:

$$k_c=\mu\omega^2(m_f/m)f+(K_{12}+T)/(\beta Q) \tag{3}$$

$$m_c^l=\mu\omega^2(m_f/m)(r_f^2+fg_1)+(M_{12}+N+bg_1T)/(\beta Qb) \tag{4}$$

$$n_c=\mu\omega^2(m_f/m)r_f^2+N/(\beta Qb) \tag{5}$$

The quantities T and N are the force and moment reactions from the balance pair attached to the flap. It is also easily seen that

$$m_c^2=m_c^l-k_cX \tag{6}$$

where $X=x_2-x_1$.

In test 3, the basic principles again yield four equations from which we find

$$k_b^i=\mu\omega^2 s_i+[\mu\omega^2(m_f/m)f-k_c]\beta/\theta+K_{i3}/(\theta Q) \tag{7}$$

$$m_b^i=\mu\omega^2 r_i^2+[\mu\omega^2(m_f/m)(r_f^2+fg_i)-m_c^i]\beta/\theta+M_{i3}/(\theta Qb) \tag{8}$$

$$n_b^i=\mu\omega^2(m_f/m)(r_f^2+fg_i)+[\mu\omega^2(m_f/m)r_f^2-n_c-C/(Qb)]\beta/\theta \tag{9}$$

C is the stiffness of the cross springs that connect the flap to the forward part in this case.

The Küssner derivatives k_a, k_b, etc. are related to the derivatives k_b^i, m_b^i, n_b^i, and m_c^i by the relations $k_b^i=-x_ik_a+k_b$, $x_ik_b^i+m_b^i=-x_im_a+m_b$, $n_b^i=-x_in_a+n_b$, and $m_c^i=-x_ik_c+m_c$, which are easily derived through superposition. Solution of k_a, k_b, etc., yields

$$k_a=-(k_b^2-k_b^l)/X \tag{10}$$

$$k_b=-(x_1k_b^2-x_2k_b^l)/X \tag{11}$$

$$m_a=-(m_b^2+x_2k_b^2-m_b^l-x_1k_b^l)/X \tag{12}$$

$$m_b=-[x_1(m_b^2+x_2k_b^2)-x_2(m_b^l+x_1k_b^l)]/X \tag{13}$$

$$m_c=m_c^i+x_ik_c \tag{14}$$

$$n_a=-(n_b^2-n_b^l)/X \tag{15}$$

$$n_b=-(x_1n_b^2-x_2n_b^l)/X \tag{16}$$

It should be mentioned that the moment signals from the balances do not represent the true moment reactions on the model, for the outer part of the balance has a nonzero moment of inertia ΔI. Due to this, a moment signal results even if no model is mounted on the balance. Hence, if N' and M_{in}' are the moments measured via the balances on the basis of a static calibration, the quantity N in Eq. (4) must be replaced by

$$N=N'+\Delta I\omega'^2\beta=N'+[\mu\omega^2(m_f/m)\Delta I/(m_fb^2)]\beta Qb \tag{17}$$

Table 2 Interference correction coefficients[a] for test section height to chord ratio 3.3 and 42% flap chord.

ω	$i=$	a Re	a Im	b Re	b Im	c Re	c Im
0.25	$c_i=$	0.908	0.065	0.910	0.066	0.913	0.058
	$d_i=$	0.918	0.051	0.915	0.039	0.828	0.016
	$e_i=$	0.904	0.101	0.946	0.107	0.954	0.054
0.40	$c_i=$	0.954	0.067	0.956	0.066	0.953	0.060
	$d_i=$	0.954	0.054	0.947	0.039	0.874	0.027
	$e_i=$	0.972	0.083	0.996	0.061	0.984	0.041
0.50	$c_i=$	0.970	0.056	0.972	0.054	0.969	0.052
	$d_i=$	0.967	0.046	0.958	0.033	0.899	0.022
	$e_i=$	0.987	0.059	0.998	0.041	0.990	0.031
0.75	$c_i=$	0.984	0.033	0.984	0.032	0.982	0.032
	$d_i=$	0.980	0.030	0.972	0.018	0.939	0.005
	$e_i=$	0.988	0.030	0.994	0.021	0.992	0.017
1.00	$c_i=$	0.985	0.021	0.984	0.021	0.984	0.021
	$d_i=$	0.982	0.020	0.978	0.009	0.960	−0.005
	$e_i=$	0.986	0.020	0.991	0.015	0.992	0.012
1.25	$c_i=$	0.984	0.016	0.984	0.015	0.984	0.016
	$d_i=$	0.983	0.015	0.981	0.004	0.972	−0.009
	$e_i=$	0.985	0.015	0.990	0.013	0.991	0.009
1.50	$c_i=$	0.984	0.012	0.984	0.012	0.983	0.012
	$d_i=$	0.983	0.012	0.984	0.002	0.980	−0.011
	$e_i=$	0.984	0.012	0.990	0.011	0.991	0.007
1.75	$c_i=$	0.984	0.010	0.984	0.010	0.983	0.010
	$d_i=$	0.983	0.010	0.987	0.000	0.985	−0.011
	$e_i=$	0.984	0.010	0.990	0.010	0.991	0.006

[a] Derivatives shall be referred to 50% chord and corrected values are obtained by multiplying measured lift, pitching moment, and flap moment by c_i, d_i, and e_i, respectively.

and the quantities M_{il} and M_{i3} in Eqs. (2) and (8) must be modified in accordance with

$$M_{in}=M_{in}'+\Delta I\omega'^2\theta=M_{in}'+[\mu\omega^2\Delta I/(mb^2)]\theta Qb \tag{18}$$

Since the value of $\Delta I/(mb^2)$ is about 0.0092, the correction is significant.

Another correction has to be made for interference due to the limited height H of the test section. Correction coefficients for this purpose were found by solving the integral equation

$$\frac{-1}{4\pi}\int_{-1/2}^{3/2}\Delta C_p(y)\left[\lim_{J\to\infty}\sum_{j=-J}^{J}(-1)^jK(y-x,jH)\right]dy = w(x) \qquad -1/2<x<3/2 \tag{19}$$

which is an extension of the well-known oscillating surface equation for two-dimensional flow. $\Delta C_p(x)$ is the dimensionless pressure jump (referred to q) across the wing and $w(x)$ the dimensionless downwash (referred to U) on the wing. The extension is obtained by considering an array of wings with separation H and alternating lift directions which produces no downwash on the tunnel floor or ceiling. The function $K(x,z)$ is defined by

$$K(x,z)=x/(x^2+z^2)+i\omega e^{i\omega x}[A(\omega z)+S(\omega x,\omega z)] \tag{20}$$

where

$$S(x,z)=\int_0^x\frac{te^{\mp it}}{t^2+z^2}dt \qquad x\gtrless 0 \tag{21}$$

and

$$A(z)=-\int_0^\infty\frac{te^{-it}}{t^2+z^2}dt=\tfrac{1}{2}[-e^{|z|}E_1(|z|)+e^{-|z|}Ei(|z|)+i\pi e^{-|z|}] \tag{22}$$

and the functions $E_1(x)$ and $Ei(x)$ are tabulated in Ref. 17.

Approximate pressure distributions and derivatives were obtained by solving Eq. (19) for $J=0$ and 9 by using the multiple lifting line method.[18] The strengths of 20 lifting lines with locations $x=-0.475(0.1)1.425$ were solved from the

linear equations that correspond to control points at $x = -0.425(0.1)1.475$. The correction coefficients, which were obtained by forming ratios of the values calculated for $J=0$ and 9 for each derivative, are given in Table 2. The use of $J=9$ instead of $J \Rightarrow \infty$ is sufficient for the present purpose.

In order to check the correction coefficients, an analogous calculation was made by solving the oscillating surface problem for an array of rectangular wings with aspect ratio 12. Four of these were arranged above and four below the primary wing with separations equal to H. The solution, which was obtained by means of a computer program based on the Polar Coordinate Method,[19] was found to agree very satisfactorily with that of the method first described.

Since the calculated correction coefficients are associated with a reference axis at 50% chord, the measured derivatives were first transformed to this axis, then multiplied by the correction coefficients, and finally transformed to the 25% chord axis. This order of operations is allowed because the forces and moments in the tunnel flow, as well as those in the unbounded flow, are linearly related to the motion of the model.

A correction should be made also for the solid blockage effect due to the thickness of the model, but this has not been applied. The correction, which can be found from Pankhurst and Holder[20] (p. 334), would reduce the magnitude of the derivatives by 1.2%.

Evaluation of the Derivatives

Equations (1-36) were used directly together with data from tests 1 and 2 for evaluation of the derivatives k_b^i, m_b^i, k_c, m_c^i, and n_c. The pitch angle θ in test 1 and the flap angle β in test 2 were considered independent real variables while the quantities K_{il} and M_{il} in test 1 and K_{i2}, T, M_{i2}, and N in test 2 were considered complex and dependent. Seven values for the modulus (magnitude) and seven values for the argument (phase angle) of each variable were recorded for each one of eight reduced frequency values.

For each frequency, a value was determined for each one of the ratios K_{il}/θ, M_{il}/θ, K_{i2}/β, T/β, M_{i2}/β, and N/β by calculating ratios of corresponding measured values and forming the arithmetic mean of the seven ratios thus obtained. The mean values were then used for the ratios in Eqs. (1-5). The constants μ, s_i, r_i^2, m_f/m, f, r_f^2, g_i, and $C/(Qb)$ which appear in the equations were put equal to the values given in Table 1.

A check of the measurement accuracy was made by plotting the magnitude of the ratios and by studying the seven primary values of the phase angle for each variable. The magnitude values formed smooth curves and the largest difference between the phase angle values for any frequency was found to be desirably small.

In test 3, the pitch angle θ was again considered real and independent, while the variables K_{i3}, M_{i3}, and β were considered complex and dependent. Attempts were made to measure the flap angle β by means of accelerometers, but the results had to be discarded because the measurement accuracy appeared unsatisfactory, particularly at the low frequencies. The values obtained for the other variables and for the ratios K_{i3}/θ and M_{i3}/θ were checked and evaluated in the same way as those in tests 1 and 2.

The attempted measurement of the flap angle was not necessary, for even the remaining measurements yield one more equation than the number of unknown quantities. Using the previously determined values for k_b^i, m_b^i, k_c, and m_c^i, the ratio β/θ was solved from both Eqs. (7) and (8). The arithmetic mean of the two results was inserted together with the previously determined value for n_c in Eq. (9) by means of which n_b^i was calculated.

The theory is based on the hypothesis that the superposition principle is applicable, which should hence be checked. Such a check has been made by varying the pitch angle in test 1 and the flap angle in test 2, the variations being 0.5-3 and 1-2 deg, respectively. The results for the derivatives, which were plotted vs the amplitude, were found to deviate very little from horizontal straight lines. It is therefore concluded that the hypothesis is satisfactory in the amplitude range considered.

Equations (10-16), which are based on the superposition principle, should hence be valid. The results for the Küssner derivatives k_a, k_b, etc., which were obtained by these formulas are collected in Table 3 and illustrated in Figs. 3-5 for k_a, m_b, and n_c.

Table 3 Experimental results for the Küssner derivatives k_a, k_b, k_c, m_a, m_b, m_c, n_a, n_b, and n_c

ω	$i=$	a Re	a Im	b Re	b Im	c Re	c Im
0.25	$k_i =$	0.148	0.379	1.435	0.193	0.888	−0.034
	$m_i =$	−0.057	0.032	−0.045	0.190	0.310	0.102
	$n_i =$	0.001	0.006	0.024	0.041	0.052	0.028
0.40	$k_i =$	0.020	0.561	1.202	0.452	0.821	0.080
	$m_i =$	−0.053	0.035	−0.081	0.287	0.303	0.171
	$n_i =$	0.001	0.025	0.008	0.064	0.049	0.051
0.50	$k_i =$	−0.048	0.557	1.100	0.619	0.784	0.155
	$m_i =$	−0.061	0.003	−0.103	0.360	0.290	0.215
	$n_i =$	−0.013	0.002	−0.000	0.081	0.044	0.063
0.75	$k_i =$	−0.289	0.763	0.898	1.065	0.712	0.342
	$m_i =$	−0.192	−0.035	−0.199	0.538	0.264	0.322
	$n_i =$	−0.036	0.009	−0.030	0.121	0.033	0.096
1.00	$k_i =$	−0.720	0.879	0.699	1.476	0.649	0.511
	$m_i =$	−0.389	−0.073	−0.324	0.724	0.226	0.429
	$n_i =$	−0.093	−0.009	−0.075	0.156	0.018	0.127
1.25	$k_i =$	−1.244	1.158	0.446	1.956	0.578	0.664
	$m_i =$	−0.650	−0.127	−0.517	0.910	0.179	0.515
	$n_i =$	−0.165	−0.017	−0.127	0.204	0.004	0.151
1.50	$k_i =$	−1.947	1.359	0.124	2.372	0.506	0.816
	$m_i =$	−0.987	−0.175	−0.739	1.079	0.113	0.622
	$n_i =$	−0.271	−0.019	−0.202	0.240	−0.019	0.181
1.75	$k_i =$	−2.187	1.563	−0.255	2.797	0.392	0.959
	$m_i =$	−1.400	−0.224	−1.012	1.246	0.019	0.704
	$n_i =$	−0.390	−0.033	−0.292	0.274	−0.053	0.203

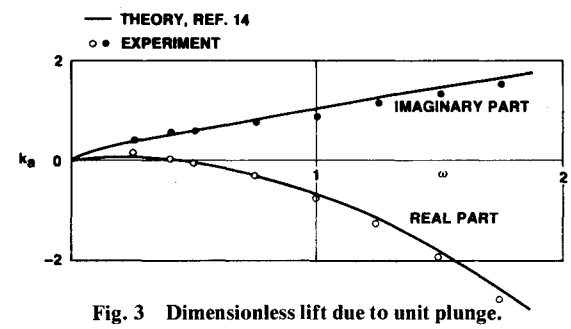

Fig. 3 Dimensionless lift due to unit plunge.

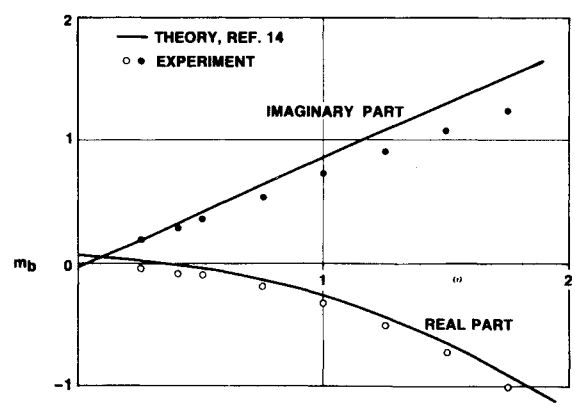

Fig. 4 Dimensionless pitching moment due to unit pitch.

Comparison with Theoretical Results for Inviscid Flow

The perturbation pressure on an oscillating profile in inviscid, incompressible, two-dimensional flow may be solved by replacing the profile contour and the wake by a polygon and by distributing sources and vortices continuously on each polygon side. This was shown by Giesing[15] who developed a

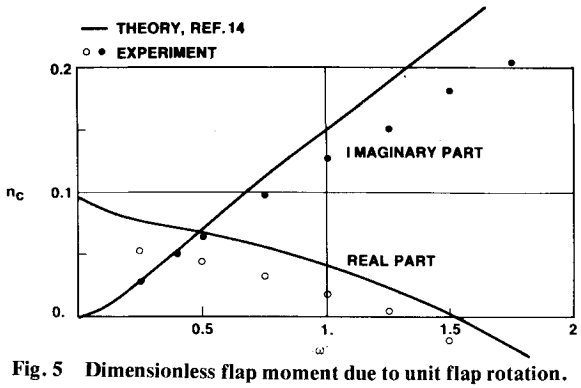

Fig. 5 Dimensionless flap moment due to unit flap rotation.

Table 4 Theoretical results for the Küssner derivatives k_a, k_b, k_c, m_a, m_b, m_c, n_a, n_b, and n_c

ω	i =	a Re	a Im	b Re	b Im	c Re	c Im
1.0	k_i =	0.000	0.000	2.230	0.000	1.677	0.000
	m_i =	0.000	0.000	0.071	0.000	0.411	0.000
	n_i =	0.000	0.000	0.069	0.000	0.097	0.000
0.2	k_i =	0.059	0.303	1.596	0.005	1.176	−0.165
	m_i =	−0.011	0.007	0.030	0.156	0.383	0.082
	n_i =	−0.002	0.009	0.046	0.034	0.079	0.021
0.5	k_i =	−0.044	0.596	1.280	0.671	0.950	0.137
	m_i =	−0.093	0.004	−0.049	0.428	0.349	0.237
	n_i =	−0.023	0.018	0.021	0.106	0.066	0.070
1.0	k_i =	−0.680	1.041	0.886	1.694	0.782	0.588
	m_i =	−0.415	−0.011	−0.279	0.877	0.273	0.497
	n_i =	−0.108	0.031	−0.046	0.223	0.041	0.151
1.5	k_i =	−1.822	1.479	0.340	2.652	0.613	0.992
	m_i =	−0.962	−0.034	−0.655	1.318	0.157	0.752
	n_i =	−0.251	0.044	−0.154	0.337	0.002	0.229
2.0	k_i =	−3.454	1.907	−0.412	3.578	0.396	1.374
	m_i =	−1.736	−0.067	−1.185	1.747	−0.007	1.003
	n_i =	−0.452	0.053	−0.305	0.447	−0.053	0.305

computer program on the basis of this approach. A similar program based on the same principle and applicable to a profile with flap without slot has been developed and applied[14] for numerical calculation of derivatives for the profile studied.

Giesing checked his program by treating a special profile and comparing the solution to a corresponding analytic solution of van de Vel.[21] He found a slight deviation, and the program of Ref. 14 also yields a similar slight deviation. The deviations, the origins of which have not yet been explained, are disturbing but not too significant. As no other more accurate method is available, the program of Ref. 14 was used for calculation of values for comparison. The calculated results are collected in Table 4 and those for k_a, m_b, and n_c are illustrated in Figs. 3-5 for comparison.

From these figures and by comparison of values from Tables 3 and 4, it is seen that the difference between the theoretical and experimental results is small to moderate for k_a, k_b, m_a, and m_b. Part of this difference may be due to viscous effects, but since minor measurement errors may remain and since the numerical solution slightly deviated from van de Vel's analytic solution, it is not certain that the viscosity is responsible for the major part.

As the boundary layer becomes thicker on the downstream part of the airfoil, it is natural to expect that the derivatives k_c, m_c, n_a, n_b, and n_c, which depend on the pressure on the downstream part, will be more affected by viscosity than the others. The difference between the theoretical and the experimental results, which appears from Fig. 5 and from comparison of values in the last row and column in Tables 3 and 4, is also seen to be larger in these cases. Probably, it is due mainly to viscous effects.

Conclusions

Unsteady aerodynamic derivatives for a NACA 64_2A015 profile with flap in two-dimensional, incompressible flow have been evaluated on the basis of data from measurements in a water tunnel at $Re = 430{,}000$. The experimental results and corresponding values calculated by a program based on inviscid, thick-wing theory differ in particular for derivatives associated with flap rotation and for flap moment due to plunge and pitch. The main part of the difference in these cases is probably a viscous effect.

Acknowledgment

The author is indebted to H. Wittmeyer, who initiated the project and led it until his retirement; to R. Frankmark and H. Kaaling (Volvo Flygmotor AB, Trollhättan) for their skillful development of test equipment and measurements; and to B. Åkerlindh and T. Ringström (Saab Scania AB, Linköping) for planning and test evaluation. The financing from the Swedish Defence Materiel Administration is also gratefully acknowledged.

References

[1] Bratt, J.B. and Scruton, C., "Measurement of Pitching Moment Derivatives for an Airfoil Oscillating about the Half-Chord Axis," British Aeronautical Research Council R&M 1921, Nov. 1938.

[2] Silverstein, A. and Joyner, U.T., "Experimental Verification of the Theory of Oscillating Airfoils," NACA Rept. 673, 1939.

[3] Reid, E.G. and Vincenti, W., "An Experimental Determination of the Lift of an Oscillating Airfoil," *Journal of Aeronautical Sciences,* Vol. 8, Nov. 1940, pp. 1-6.

[4] Reid, E.G., "Experiments on the Lift of Airfoils in Nonuniform Motion," Stanford University Report, July 23, 1942.

[5] Bratt, J.B. and Wight, K.C., "The Effect of Mean Incidence, Amplitude of Oscillation, Profile, and Aspect Ratio on Pitching Moment Derivatives," British Aeronautical Research Council R&M 2064, June 1945.

[6] Halfman, R.L., "Experimental Aerodynamic Derivatives of a Sinusoidally Oscillating Airfoil in Two-Dimensional Flow," NACA TN 2465, Nov. 1951.

[7] Drescher, H., "Eine Experimentelle Bestimmung der Aerodynamischen Reaktionen auf einen Flügel mit Schwingendem Ruder," *Österreichisches Ingenieur-Archiv,* Vol. IV, No. 3-4, 1950.

[8] van de Vooren, A.I., "Measurement of Aerodynamic Forces on Oscillating Aerofoils," AGARD Paper 15/PG, 1954.

[9] Bergh, H., "Experimental Determination of Aerodynamic Coefficients of Vibrating Wings," NAL, Amsterdam, March 1957, NASA TT F-81, Sept. 1963, pp. 106-131.

[10] Küssner, H.G., "Der schwingende Flügel mit aerodynamisch ausgeglichenem Ruder," *Luftfahrtforschung,* Vol. 17, Dec. 1940, pp. 337-354.

[11] Theodorsen, T., "General Theory of Aerodynamic Instability and the Mechanism of Flutter," NACA Rept. 496, 1935.

[12] Spurk, J., "Messungen der aerodynamischen Beiverte schwingender Flügelprofile im Windkanal und Vergleich mit der Theorie," Max-Planck-Institut für Strömungsforschung und der Aerodynamischen Versuchsanstalt, Göttingen, Mitteilung Nr. 29, 1963.

4[13] Küssner, H.G., "Theorie des instationär bewegten Flügelprofils endlicher Dicke," *Zeitschrift für Flügwissenschaften,* Vol. 9, 1961, pp. 106-112.

[14] Stark, V.J.E., "Calculation of Forces and Moments on an Oscillating NACA 64_2A015 Profile with Flap," Saab-Scania AB, Linköping, Rept. FKLF-0-78:26, April 1978.

[15] Giesing, J.P., "Two-dimensional Potential Flow Theory for Multiple Bodies in Small-Amplitude Motion," McDonnell Douglas Rept. DAC-67028, April 1968.

[16] Drescher, H., "Neue Wasserkanäle der AVA," *Jahrbuch 1941 der deutschen Luftfahrtforschung,* pp. I714-I722.

[17] Gautschi, W. and Cahill, W.F., "Exponential Integral and Related Functions," *Handbook of Mathematical Functions with Formulas, Graphs, and Mathematical Tables,* edited by M. Abramowitz, and I.A. Stegun, National Bureau of Standards Applied Mathematics Series 55, 9th printing, Nov. 1970, pp. 227-251.

[18] Landahl, M.T. and Stark, V.J.E., "Numerical Lifting-Surface Theory – Problems and Progress," *AIAA Journal,* Vol. 6, Nov. 1968, pp. 2049-2060 (see also p. 2055).

[19] Stark, V.J.E., "Application to the Viggen Aircraft Configuration of the Polar Coordinate Method for Unsteady Subsonic Flow," Paper 74-03 presented at 9th Congress of the International Council of the Aeronautical Sciences, Haifa, Aug. 1974.

[20] Pankhurst, R.C. and Holder, D.W., *Wind-Tunnel Technique,* Sir Isaac Pitman & Sons, Ltd., London, 1952.

[21] van de Vel, H., "Unsteady Profile Theory in Incompressible Flow," Thesis, University of Groningen, the Netherlands, 1964.